The molecular basis of human 3-methylcrotonyl-CoA carboxylase deficiency

Matthias R. Baumgartner,[1,2] Shlomo Almashanu,[1,3] Terttu Suormala,[2] Cassandra Obie,[1,3] Robert N. Cole,[4] Seymour Packman,[5] E. Regula Baumgartner,[2] and David Valle[1,3]

[1]McKusick-Nathans Institute of Genetic Medicine, Johns Hopkins University, Baltimore, Maryland, USA
[2]Metabolic Unit, Children's Hospital, University of Basel, Basel, Switzerland
[3]Howard Hughes Medical Institute, and
[4]Department of Biological Chemistry, Johns Hopkins University, Baltimore, Maryland, USA
[5]Department of Pediatrics, University of California, San Francisco, California, USA

Address correspondence to: David Valle, 802 PCTB,
Johns Hopkins University, 725 N. Wolfe Street, Baltimore, Maryland 21205, USA.
Phone: (410) 955-4260; Fax: (410) 955-7397; E-mail: dvalle@jhmi.edu.

Received for publication December 6, 2000, and accepted in revised form January 7, 2001.

Isolated biotin-resistant 3-methylcrotonyl-CoA carboxylase (MCC) deficiency is an autosomal recessive disorder of leucine catabolism that appears to be the most frequent organic aciduria detected in tandem mass spectrometry–based neonatal screening programs. The phenotype is variable, ranging from neonatal onset with severe neurological involvement to asymptomatic adults. MCC is a heteromeric mitochondrial enzyme composed of biotin-containing α subunits and smaller β subunits. Here, we report cloning of MCCA and MCCB cDNAs and the organization of their structural genes. We show that a series of 14 MCC-deficient probands defines two complementation groups, CG1 and 2, resulting from mutations in *MCCB* and *MCCA*, respectively. We identify five *MCCA* and nine *MCCB* mutant alleles and show that missense mutations in each result in loss of function.

J. Clin. Invest. **107**:495–504 (2001).

Introduction

MCC (EC 6.4.1.4) is a biotin-dependent carboxylase that catalyzes the fourth step in the leucine catabolic pathway. Isolated, biotin-resistant MCC deficiency (also known as methylcrotonylglycinuria [MIM 210200]) is inherited as an autosomal recessive trait (1). The clinical phenotype is highly variable: some patients present in the neonatal period with seizures and muscular hypotonia (2, 3); others are asymptomatic women identified only by detection of abnormal metabolites in the neonatal screening samples of their healthy babies (4). There is a characteristic organic aciduria with massive excretion of 3-hydroxyisovaleric acid and 3-methylcrotonylglycine, usually in combination with a severe secondary carnitine deficiency. MCC activity in extracts of cultured fibroblasts of patients is usually less than 2% of control. No correlation between the level of residual enzyme activity and clinical presentation has been observed.

Tandem mass spectrometry (MS/MS), recently introduced for newborn screening, provides for the first time to our knowledge a way to detect a large variety of organic acidurias including MCC deficiency (5). Surprisingly, MCC deficiency appears to be the most frequent organic aciduria detected in MS/MS screening programs in North America (4, 6, 7), Europe (8), and Australia (9), with an overall frequency of approximately 1 in 50,000.

MCC is a member of the family of biotin-dependent carboxylases, a group of enzymes with diverse metabolic functions but common structural features (10, 11). Members of this family have three structurally conserved functional domains: the biotin carboxyl carrier domain, which carries the biotin prosthetic group; the biotin carboxylation domain, which catalyzes the carboxylation of biotin; and the carboxyltransferase domain, which catalyzes the transfer of a carboxyl group from carboxybiotin to the organic substrate specific for each carboxylase (10, 12). In addition to MCC, there are three other biotin-dependent carboxylases in humans: propionyl-CoA carboxylase (PCC), pyruvate carboxylase (PC), and acetyl-CoA carboxylase (ACC) (10, 11). The genes for all human carboxylases except MCC have been cloned and characterized (13–15).

MCC carboxylates 3-methylcrotonyl-CoA at the 4-carbon to form 3-methylglutaconyl-CoA (Figure 1) (1). The reaction uses ATP and bicarbonate and is reversible. Bovine MCC has an approximate size of 835 kDa and appears to comprise six heterodimers $(\alpha\beta)_6$ (16). Like PCC, MCC has a larger α subunit, which covalently binds biotin, and a smaller β subunit (13). MCC is predominantly localized to the inner membrane of mitochondria and is known to be highly expressed in kidney and liver (1). cDNAs encoding both subunits of MCC recently have been cloned in *Arabidopsis thaliana* and other plants (17, 18).

Here we report cloning of human *MCCA* and *MCCB* cDNAs, confirmation of their identity by biochemical and molecular studies, and identification of mutations in MCC-deficient patients.

Methods

Patients, complementation analysis, and MCC assay

This study includes 16 MCC-deficient probands, all of whom had the diagnostic pattern of organic acid excretion and less than 10% MCC activity in extracts of cultured skin fibroblasts. Clinical and biochemical data of ten patients have been reported in the literature: 001 (3), 002 (2), 003 (19), 004 (20), 006 (21), 007 (22), 010 (23), 011 (24), 012 (25), and 016 (4). Fibroblasts or DNA of the remaining patients were referred by B.T. Poll-The (patient 005), H.G. Koch (patient 008), J. Smeitink (patient 009), U. von Döbeln (patient 013), R.D. De Kremer Dodelson (patient 014), and D.H. Morton (patient 015). Skin fibroblasts were cultured in Eagle's minimal essential medium (Life Technologies Inc., Rockville, Maryland, USA) supplemented with 2 mmol/l L-glutamine and 10% FCS. Complementation analysis was modified from that described by Wolf et al. (26). Briefly, we produced heterokaryons by a 90- or 120-second treatment with 40% PEG harvested the cells 3 days later and measured MCC activity as described previously (3, 27). MCC activity in cultures of mixed but unfused cells was subtracted as blank and self fusions were included as a negative control.

Expression of biotin-containing proteins in fibroblasts

We harvested cultured fibroblasts by trypsinization, disrupted the washed cells by homogenization, harvested the mitochondria by differential centrifugation (28), suspended them in SDS-buffer (50 mM Tris-acetate, 1% SDS [wt/vol], 10 mM DTT, 0.02% [wt/vol] bromphenol blue), and dissolved the proteins by boiling for 5 minutes. The cellular proteins were separated by SDS-PAGE, and the biotin-containing proteins were detected with an avidin alkaline phosphatase conjugate (avidin-AP, 1:8,000; Bio-Rad Laboratories AG, Glattbrugg, Switzerland).

Fibroblasts of an unaffected control, a patient with isolated PC deficiency, and a patient with isolated PCCα deficiency were used to confirm the identity of the protein bands.

cDNA cloning, sequence analysis, and chromosome mapping

We obtained two mouse (AI317324 and AI117072) and two human (AA134548 and AA101775) *MCCA* EST clones, and one human *MCCB* (AI564487) EST clone from the IMAGE consortium (Genome Systems Inc., St. Louis, Missouri, USA) and sequenced both strands with an ABI 377 automated sequencer. To design primers corresponding to the 5′ UTR of our putative *MCCA*, we used the sequence of the *MCCA* EST clone AA337013 (not available commercially). We used primers DV4418 (sense, 5′-GACGCAGCTGCCTCTG TAC) and DV4417 (sense, 5′-TGGCCGGGCTCCAGGGACATG), complementary to the 5′ UTR, and DV4446 (antisense, 5′-AACTGCTCTTTATGAGACCCC), complementary to the 3′ UTR, to amplify full-length human *MCCA* from a human retina cDNA library (29); and primers DV4496 (sense, 5′-AGGACCTGAGCTCAGCTTCC) and DV4497 (sense, 5′-TCGGTGCCCGCCGCCATG), complementary to the 5′ UTR, and DV 4495 (antisense, 5′-ACTG-TAACAGCCTCATGTTCG), complementary to the 3′ UTR, to amplify full-length human *MCCB* from the same human retina cDNA library (29). We gel-purified the PCR products and sequenced them directly. The sequence alignments were prepared with MegAlign (DNASTAR Inc., Madison, Wisconsin, USA).

We mapped *HsMCCA* using the Genebridge 4 radiation hybrid panel (Research Genetics Inc., Huntsville, Alabama, USA) using primers DV4621 (sense, 5′-TTTGTCGTCTCAGACTCGATG) and DV4740 (antisense, 5′-AGTCAGAAAAATAAGGCCAACC) corresponding to 5′ flanking intronic sequence of exon 6 and 3′ flanking intronic sequence of exon 7.

Isolation and mass spectrometry analysis of biotin-containing proteins

Enrichment for biotin-containing proteins. We homogenized 0.32 g of flash frozen male mouse kidney in 1.5 ml buffer A (100 mM Tris-HCl [pH 7.4], 20 mM DTT, 1 mM EDTA, 0.1% (vol/vol) Triton X-100, 20% (vol/vol) glycerol, 1 μM DMSF, 1 tablet cocktail protease inhibitor (Boehringer-Mannheim) and centrifuged the homogenate at 20,000 *g* for 20 minutes at 4°C. PEG was added to the supernatant to a final concentration of 16% (wt/vol), and the mixture was centrifuged at 20,000 *g* for 30 minutes at 4°C. The pellet was resuspended in 1 ml of buffer A, approximately 3×10^8 prewashed M280 streptavidin Dynabeads (Dynal Inc., Lake Success, New York, USA) were added, and the slurry mixed by rotating for 1 hour at 4°C. We washed the beads five times with buffer B (0.25 M KCl in buffer A), resuspended them in 200 μl of XI protein loading buffer, boiled for 5 minutes, and placed the solution on ice. We loaded 25 μl in each lane of a 10% polyacrylamide gel and stained the separated proteins with Coomassie Brilliant blue R250.

S-carboxymethylation and proteolytic digestion. We performed in gel digestion of the proteins using the Coomassie blue–stained SDS-polyacrylamide gels according to Williams et al. (30) with the following modifications. Cystines were modified by carboxymethylation as described elsewhere (31). After rehydrating gel pieces with 5 ng/μl TPCK-treated trypsin in 1% acetic acid, excess trypsin solution was removed and the gel piece was covered with 2 gel volumes of 200 mM NH4HCO3 (pH 8), at 37°C for 48 hours. The resulting tryptic peptides were extracted from the gel piece with 60% acetonitrile in 0.1% TFA and concentrated by drying.

Mass spectrometry analysis. Tryptic peptides were resuspended in 1% acetic acid and loaded into a fused silica capillary column (75 μm inner diameter) packed with 10 cm of 5 μm C18 reverse-phase resin (YMC Inc., Atlanta, Georgia, USA) as described elsewhere (32). A

30-minute, 1.5–70% methanol gradient in 1% acetic acid was applied to the column at flow rates of 250–300 nl/min. Eluting peptides were electrosprayed directly into a Finnigan LCQ atmospheric pressure ionization quadrupole ion trap mass spectrometer (ThermoQuest Corp., San Jose, California, USA). Positive-ion mass spectra were obtained at using XCalibur software (ThermoQuest Corp.). Peptides were fragmented by a 35% collision energy using a two-atomic-mass-unit isolation width. Fragmentation data were screened against the protein.nrdb.Z database from the Frederick Biomedical Supercomputing Center (ftp://ftp.ncifcrf.gov/pub/nonredun/) using the SEQUEST Browser (33) (ThermoQuest Corp.).

Mutation analysis by RT-PCR and genomic PCR

We extracted RNA and genomic DNA from cultured skin fibroblasts and/or blood using the Puregene RNA and DNA isolation kits (Gentra Systems, Minneapolis, Minnesota, USA) and performed RT-PCR using 5–10 μg fibroblast RNA and a cDNA cycle kit (Invitrogen Corp., Carlsbad, California, USA) following the manufacturers' recommendations. We generated first-strand cDNA with primers DV4403 (antisense, 5′-GACCCAAATGCATGATTCTCC), complementary to sequence in the MCCA 3′ UTR region, and DV 4506 (antisense, 5′-GGTAGAAAAGTACAA TGCACAG), complementary to sequence in the MCCB 3′ UTR region. We then amplified first-strand MCCA cDNA with primers DV4418 and DV4446 to generate a 2,326-bp fragment (–51 to +2275, where +1 is the A of the initiation methionine codon); and we amplified first-strand MCCB cDNA with primers DV4496 and DV 4495 to generate a 1,923-bp fragment (–99 to +1824). In some instances, when the amount of amplified product was inadequate, we went through a second round of PCR with nested primers DV4417 and DV4497. We gel-purified the PCR products and sequenced them directly.

To confirm mutations identified in RT-PCR products, we amplified a genomic fragment containing the corresponding exon using flanking intronic primers and sequenced the PCR product directly. In the compound heterozygous patients in whom we identified only one of two alleles in RT-PCR products, we amplified and sequenced all exons and flanking intronic sequences.

All PCR reactions (50 μl) contained primers (100 ng each), 1× standard PCR buffer (Life Technologies Inc.), dNTPs (200 μM), and *Taq* polymerase (2.5 U; Life Technologies Inc.). The sequences of all primers are available upon request.

To survey a control population for the identified missense mutations, we amplified the relevant exon from genomic DNA and performed allele-specific oligonucleotide analysis as described previously (34).

Construction of wild-type and mutant human MCCA/B expression vectors

We TA cloned the full-length human MCCA (–51 to +2275) and MCCB (–99 to +1824) cDNAs into pCR Blunt II TOPO (Invitrogen Corp.). To introduce the *MCCA* mutations R385S, A289V, and L437P, we harvested an 896-bp *ACC*I fragment from RT-PCR–amplified patient cDNA and subcloned this fragment into the pMCCA-TOPO construct. We then transferred the wild-type and mutant MCCA constructs into a mammalian expression vector (pTracer-CMV2; Invitrogen-Corp.) at the *EcoR* I site. This vector contains a green fluorescent protein (GFP) gene fused to the Zeocin resistance gene. Similarly, to introduce the *MCCB* missense mutation E99Q, we harvested a 193-bp *EcoN* I/*BstE* II fragment from RT-PCR amplified patient cDNA, subcloned this fragment into the pMCCB-TOPO construct and then transferred the wild-type and mutant constructs into pTracer-CMV2. To introduce the *MCCB* missense mutations S173L, V339M, R155C, P310R and R193C, we harvested a 965-bp *BstE* II/*Sfi* I fragment from RT-PCR–amplified patient cDNA and subcloned this fragment directly into MCCB-pTracer-CMV2. We sequenced all constructs in both directions to validate the sequences.

Transfections

We transformed primary fibroblasts from proband 010 (homozygous for *MCCA* Q421fs(+1), from proband 001 (homozygous for *MCCB* S173L), and from a control as described previously (34). For expression studies, we electroporated the indicated constructs into transformed cells as described elsewhere (34). We harvested the cells after 72 hours and measured MCC and PCC activity radioisotopically as described previously (27). Our standard MCC assay enables us to reliably detect activity as low as 5–10 pmol/min/mg protein. All

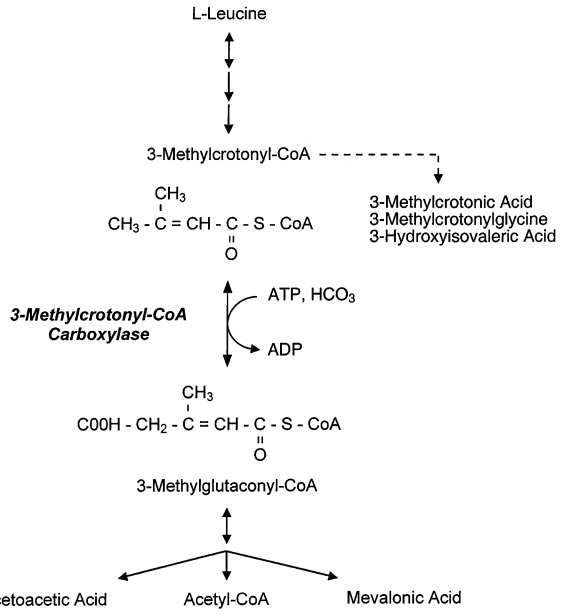

Figure 1
The MCC-catalyzed reaction and its position in the leucine catabolic pathway. The dashed arrow indicates the metabolites that accumulate due to deficiency of MCC.

transfections were in duplicates. Transformed fibroblasts from an unaffected individual were used as control. Transfection efficiency was assessed by coexpressing GFP in the same construct.

Results

Genetic complementation and assignment to *MCCA* or *MCCB*

As an initial step in defining the molecular basis of MCC deficiency, we performed biochemical and somatic cell genetic studies with fibroblasts from 14 MCC-deficient probands. Using restoration of MCC activity in PEG-induced heterokaryons of fibroblasts as an end point, we defined two complementation groups (CGs), one comprising eight probands (MCC-CG1, 001-008) and the other, six probands (MCC-CG2, 009-014) (data available upon request). Given that MCC is composed of αβ heteromers, we anticipated that the two CGs likely corresponded to mutations in genes encoding the α and β subunits of MCC (encoded by *MCCA* and *MCCB*, respectively).

To investigate the complementation phenotype at the protein level, we examined the expression of the MCCα subunit using the covalently bound biotin as a tag in fibroblasts of five of six CG2 and in all of the eight CG1 probands (Figure 2). In CG2, MCCα was not detected in four of five probands, whereas in the remaining CG2 cell line (proband 011), the MCCα band was at least as intense as in controls (Figure 2). In all the CG1 cell extracts, MCCα was reduced but present. These results suggested that MCC-CG2 is caused by mutations in *MCCA* and, by exclusion, MCC-CG1, by mutations in *MCCB*.

Identification of mammalian candidate MCCA and MCCB cDNAs

Database search. We used the amino acid sequences of *A. thaliana MCCA* and *MCCB* (17, 18) and the TBLASTN algorithm to probe the public EST databases to identify murine and human cDNAs encoding candidate MCCAs and MCCBs. We used the murine candidates to assemble full-length mouse putative MCCA cDNA (GenBank accession number: *MmMCCA*: AF310338) and the human candidate ESTs to design primers corresponding to the predicted 5′ and 3′ UTR of the putative human MCCA and MCCB cDNAs. Using these primer pairs, we amplified a single fragment of the predicted size for both MCCA and MCCB from a human retina cDNA library (29). GenBank accession numbers: *HsMCCA*: AF310339. *HsMCCB*: AF301000. We used additional ESTs to extend the 5′ and 3′ UTR sequences. The sequence of the human MCCA candidate has 57 bp of 5′ UTR, a 2,175-bp ORF, and 222 bp of 3′ UTR extending to a polyadenylation signal (AAUAAA). The murine candidate MCCA cDNA has 42 bp of 5′ UTR, a 2,151-bp ORF, and 190 bp of 3′ UTR extending to a probable polyadenylation signal (AUAAA). The sequence of the amplified human MCCB candidate has 99 bp of 5′ UTR, a 1,689-bp ORF, and 540 bp of 5′ UTR.

The candidate cDNAs predict a human MCCα of 725 amino acids with a calculated molecular mass of 80 kDa, a mouse MCCα of 717 amino acids with a calculated molecular mass of 79 kDa, and a human MCCβ of 563 amino acids with a calculated molecular mass of 61 kDa. Human MCCα has 84% and 45% identity to MCCα of mouse and *A. thaliana*, respectively (Figure 3a). Human MCCβ has 60% identity to MCCβ of *A. thaliana* (Figure 3b). Similar to PCC, the MCCα subunit contains an NH_2-terminal biotin carboxylation domain and a COOH-terminal biotin carrier domain (10). The biotin carrier domain is centered on the motif AMKM, which is found in most biotinylated proteins (Figure 3a) (10). Biotin is covalently attached to the ε-amino group of lysine 681; the ε-biotinyl lysine amide is termed biocytin (Figure 3a). As with other biotin-dependent carboxylases, there is a conserved (A)PM motif 29 residues NH_2-terminal and a hydrophobic residue (F714) 33-31 residues COOH-terminal of biocytin (35). The biotin carboxylation domain is located in the NH_2-terminal two-thirds of MCCα and is linked to the biotin carrier domain by a less-conserved (only 25% identity to *A. thaliana* residues 427-664) "hinge" region of residues 441-650. Additionally, there is perfect conservation of 11 residues (Figure 3a, asterisks) that are highly conserved among all biotin-dependent

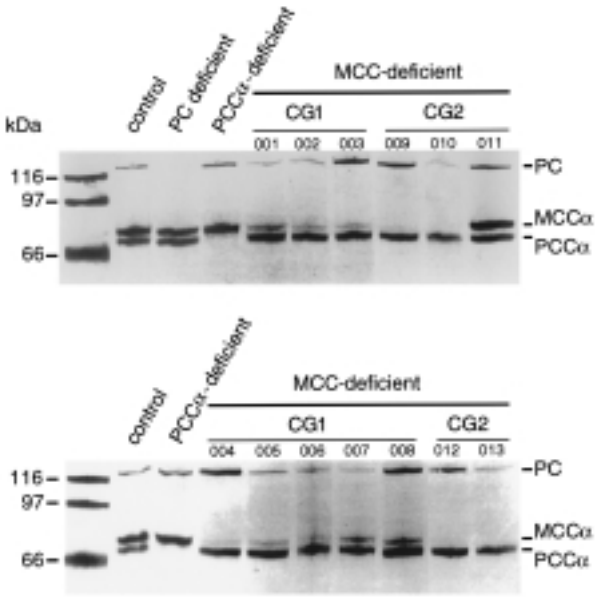

Figure 2
Expression of the biotin-containing MCCα subunit in fibroblasts. Proteins in mitochondrial enriched fractions from cultured fibroblasts were separated by SDS-PAGE, and the biotin-containing subunits of MCC, PCC, and PC were detected with an avidin alkaline phosphatase conjugate. Most, but not all, CG2-probands lack the MCCα subunit, while it is detectable in all CG1 probands.

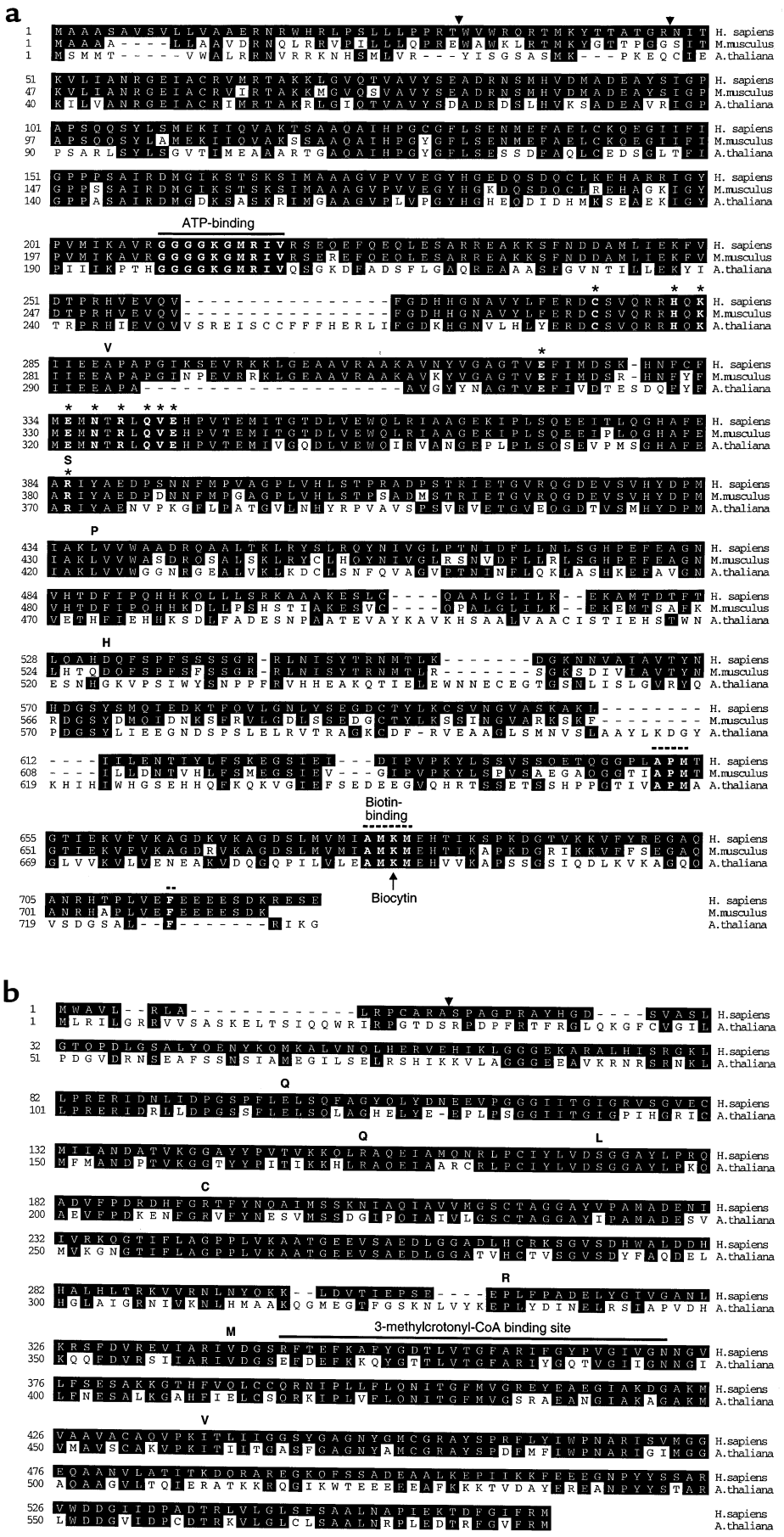

Figure 3
Sequence alignment of human MCCα and MCCβ with orthologs from mouse and *A. thaliana*. Amino acids identical to the human sequence are highlighted. Missense mutations identified in MCC-deficient patients are indicated above with the substituted amino acid. Potential cleavage sites for the NH_2-terminal mitochondrial leader sequences are indicated by vertical arrowheads. (**a**) Sequence alignment of human, mouse, and *A. thaliana* MCCα. The predicted ATP-binding site in the NH_2-terminal biotin carboxylation domain and the predicted COOH-terminal biotin carboxyl carrier domain are indicated by solid and dashed overlines, respectively. The arrow indicates the lysine residue that links covalently to biotin (biocytin). The residues marked with an asterisk within the biotin carboxylation domain are thought to play an important role in catalysis (36, 37). (**b**) Sequence alignment of human and *A. thaliana* MCCβ. The putative 3-methylcrotonyl-CoA binding domain is indicated by a solid over-line.

carboxylases and thought to play a role in catalysis (12, 36, 37). Consistent with this prediction, the putative carboxylation domain contains the conserved sequence GGGGKGMRIV at positions 209-218 (Figure 3a), which is part of the ATP binding pocket in the biotin carboxylation domain of *Escherichia coli* ACC (37) and is similar to a consensus P-loop ATP-binding site [G′XGK(TS)] (38). The β subunit has a putative CoA binding motif (Figure 3b) (10, 39).

MCCα and β have candidate NH_2-terminal mitochondrial targeting sequences with multiple arginine residues and a paucity of acidic residues (40). Possible cleavage sites are indicated by vertical arrowheads in Figure 3. Because the sequence of mitochondrial leaders is not highly conserved, we favor the more COOH-terminal cleavage site in MCCα just before a highly conserved region (Figure 3a).

Isolation and mass spectrometry analysis of biotin-containing proteins. We also used a biochemical strategy to identify MCCα and β. We enriched biotin-containing proteins in a mouse kidney extract using streptavidin Dynabeads and separated these by SDS-PAGE (Figure 4). Using MALDI-TOF and electrospray ionization mass spectrometry (ESI-MS/MS), we analyzed tryptic fragments of these proteins to confirm the identity expected on the basis of the size of ACC, PC, and PCCβ. The analysis of the expected PCCα identified, in addition to fragments derived from PCCα, unique fragments corresponding to the conceptual translation of the putative murine MCCA cDNA (Figure 4). We identified 35 peptides with 100% identity to the putative murine MCCα subunit covering 571 amino acids or 80% of the putative full-length murine MCCα. The protein comigrating with the 66-kDa marker (Figure 4) contained tryptic fragments with sequences corresponding to the conceptual translation of the putative human MCCB cDNA. We identified 25 peptides with 100% identity to the putative human MCCβ subunit covering 414 amino acids or 74% of the putative full-length MCCβ. These sequence results strongly supported the identity of the mammalian MCCA and MCCB cDNAs.

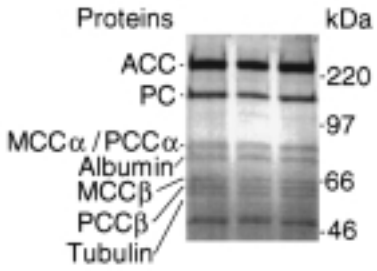

Figure 4
Coomassie-stained SDS-PAGE gel of biotin-containing proteins purified from a mouse kidney extract with streptavidin Dynabeads. We excised the proteins from the gel, digested with trypsin, and analyzed the tryptic peptides using MALDI-TOF and liquid chromatography coupled to ESI-MS/MS. We analyzed all the indicated bands including those that we identified as MCCα and β.

Organization of human *MCCA* and *MCCB* structural genes

During the course of determining the structural organization of these genes by long-range PCR and direct sequencing, we identified sequences corresponding to *MCCA* and *MCCB* in the human high throughout genome sequence database (GenBank accession numbers AC026920 and AC026775, respectively). These clones contain exons encoding the complete MCCA and MCCB cDNAs and provide all exon/intron boundaries including the flanking intronic sequences with one exception (5′ flanking intronic sequence of *MCCA* exon 8). *MCCA* has 19 exons and *MCCB* 17 exons. Given that the draft sequence has gaps, our information on the size of some introns is incomplete.

Because the *MCCA* gene was not mapped in the UniGene database, we searched the flanking sequence in the BAC clone containing *MCCA* for other mapped genes. We identified the UniGene cluster Hs.10887 represented by several ESTs present in the *MCCA* genomic clone and localized to 3q25-q27 (*D3S1553-D3S1580*). To confirm this localization, we used the Genebridge 4 radiation hybrid panel to regionally localize *MCCA* 3.56 cR from the WI-6365 marker corresponding to the same region on chromosome 3. Similarly, we identified UniGene cluster Hs.167531 representing several EST clones covering the 3′ end of the MCCB cDNA. This cluster maps to chromosome 5q12-q13.1 (*D5S637-D5S1977*).

Patients with isolated MCC deficiency have mutations in *MCCA* or *MCCB*

To confirm the identity of *MCCA* and *MCCB*, we surveyed these genes for mutations in our collection of 14 unrelated MCC-deficient probands. We grouped the probands according to their CGs and used RT-PCR to amplify the corresponding mRNA from their cultured skin fibroblasts. We sequenced the entire ORF in each proband and confirmed all mutations by direct sequencing of PCR-amplified genomic DNA. In two additional probands (015 and 016) (ref. 4) from the Amish/Mennonite population in Lancaster County, Pennsylvania, we searched for mutations by direct sequencing of PCR-amplified genomic DNA. We identified five *MCCA* mutant alleles in CG2 cell lines accounting for ten of 12 possible mutant *MCCA* genes (Table 1). The mutations include three uncomplicated missense mutations (Figure 3a), one missense mutation that alters splicing (Figure 5a), and one 1-bp insertion. In CG1 cell lines, we identified nine *MCCB* mutant alleles accounting for 12 of 16 possible mutant genes (Table 2). The mutations include 6 uncomplicated missense mutations (Figure 3b), one missense mutation that alters splicing (Figure 5b), one splice site mutation, and one 1-bp insertion. In spite of sequencing all exons and flanking intronic sequences (with the exception of the

5′ flanking intronic sequence of *MCCA* exon 8), we were not able to identify a second allele in two CG2 and four CG1 probands. In five of these probands, the one allele identified appeared to be homozygous in the RT-PCR product, but was clearly heterozygous in genomic DNA, suggesting that the steady level of mRNA from the second allele was not detectable as would be the case for a promoter mutation or an intragenic deletion or insertion missed by genomic PCR. These results strongly support the identification of the *MCCA* and *MCCB* genes and their assignment to MCC deficiency in CG2 and CG1, respectively.

Expression of *MCCA* and *MCCB* alleles

As a final test of the identity of our candidate human MCCA and MCCB cDNAs, we subcloned them into a mammalian expression vector (pTracer-CMV2), electroporated the recombinant constructs into a SV40T transformed reference CG2 or CG1 cell line, and measured MCC activity 72 hours later (27). As a reference, we also measured PCC activity (27). Wild-type *MCCA* and *MCCB* alleles restored MCC activity to 43% and 53% of untransfected control fibroblasts, respectively (Table 3). Transfection efficiency, assessed by scoring a subset of cells in each transfection for the presence of the coexpressed GFP, ranged from 10 to 20% in these experiments.

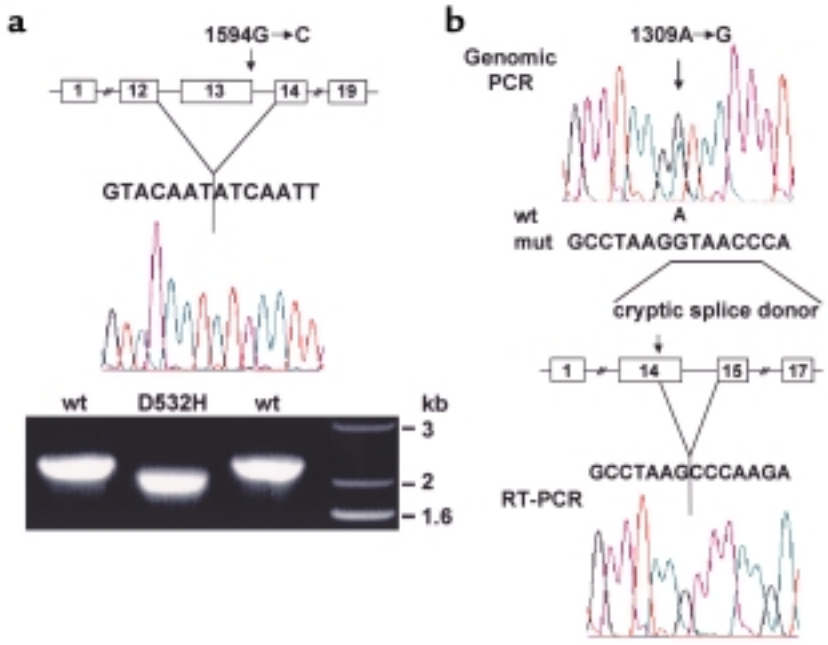

Figure 5
MCCA and *B* missense mutations that alter splicing. (**a**) *MCCA* D532H. The 1594G→C transversion of the last bp of exon 13 results in the missense mutation D532H. The 3′ base of an exon also contributes to donor splice site recognition and, as shown in the lower panel, RT-PCR of MCCA cDNA in this patient with primers corresponding to the 5′ and 3′ UTR resulted in a product smaller than in wild-type. Sequence analysis of this product showed that exon 13 (217 bp) is skipped, which shifts the reading frame. Thus, the deleterious consequences of this missense mutation appear to be entirely due to the splicing defect. (**b**) *MCCB* I437V. As shown in the upper panel, the 1309A→G transition in exon 14 results in the replacement of isoleucine by valine, a conservative change. However, the mutation also activates a cryptic splice donor. Use of this new donor splice site deletes the last 64 bp of exon 14 from the mature transcript. As shown in the lower panel, direct sequencing of the RT-PCR product shows that virtually all the transcript present uses the new, more 5′ splice donor. The second allele of this compound heterozygous patient does not produce detectable RNA. wt, wild-type; mut, mutant.

Similarly, to test the functional consequences of the missense mutations, we expressed three *MCCA* and six *MCCB* missense alleles. *MCCB*-R193C and -V339M had activity of 6 and 7 pmol/min/mg protein, respectively, or about 4% of the activity produced by the wild-type allele, whereas the remaining four *MCCB* alleles and the three *MCCA* alleles produced no detectable activity (Table 3). These results confirm the deleterious functional consequences of the tested missense mutations.

Population frequency of selected *MCCA* and *MCCB* alleles

Additionally, we used allele-specific oligonucleotide analysis (34) to survey a North American control population of 66 individuals for three *MCCA* alleles (R385S, A289V, and L437P) and two *MCCB* alleles (E99Q and R193C). Aside from one individual heterozygous for R385S, we did not identify any of these alleles in this collection of 132 control chromosomes (data not shown). These results indicate that each of these mutant alleles has a low frequency in this population. We did not screen for alleles for which we did not have the appropriate control population (Vietnamese, *MCCB*-R155Q, -P310R; Turkish, *MCCB*-S173L, -V339M).

Discussion

Using a combination of homology probing and mass spectrometry we cloned human MCCA and MCCB full length cDNAs. The conceptual translation of *MCCA* shows the expected NH_2-terminal biotin carboxylation domain and the COOH-terminal biotin carboxyl carrier domain (Figure 3a), separated by a less conserved "hinge" region (10, 12). Presumably because of differences in substrate specificities, carboxyltransferase domains are less conserved among biotin-dependent carboxylases. MCC catalyzes the carboxylation of methylcrotonyl-CoA (1). The acceptor binding site is thought to be on MCCβ (10, 39). Consistent with this, human MCCβ shares high identity with *A. thaliana* MCCβ (60%) and only 28% identity with human PCCβ (13) that supports the role of the β subunit in determining substrate specificity of these enzymes (Figure 3b).

Our series of 6 *MCCA*- and 10 *MCCB*-deficient

Table 1
MCCA mutant alleles

No.	Allele	Exon	Nucleotide change	Clinical phenotype[A]	Ethnic origin	Proband
1	R385S	11	1155A→C	Severe	German	011[B]
2	Q421fs(+1)	11	1264insG	Mild	Swedish/Amer.	013[C], 010[B]
3	A289V	8	866C→T	Mild	American	012[C]
4	D532H	13	1594G→C[D]	Severe	Turkish	009[B]
5	L437P	12	1310T→C	Severe	Argentine	014[B]

[A]Mild: late onset, good recovery after acute attack, no or mild developmental delay; severe: onset in infancy, severe neurological involvement with severe developmental delay. [B]Homozygous. [C]Only one allele identified. [D]Alters splicing (Figure 5a).

probands is characterized by the fact that almost every proband had a unique genotype with no prevalent mutant allele for either gene. In agreement with this observation, using allele-specific oligonucleotide analysis to screen 66 North American controls (132 chromosomes), we found only a single heterozygote from one allele (*MCCA*-R385S) and no carriers for the others tested (*MCCA*-A289V, -L437P; *MCCB*-E99Q, -R193C). For *MCCA*, we assume functional significance for the frameshift mutation Q421fs(+1) and the missense mutation D532H, which alters splicing (Figure 5a), because both result in truncated proteins lacking functionally important domains. The *MCCA* mutations R385S, A289V, and L437P all change conserved residues (Figure 3a), and the corresponding alleles confer no detectable MCC activity when expressed in the CG2 reference cell line (Table 3). In contrast to the other four CG2 probands tested, who had no detectable MCCα, we detected normal amounts of MCCα protein in the proband 011 homozygous for R385S (Figure 2). This result is consistent with the prediction based on the structure of the biotin carboxylation domain of *E. coli* ACC that the residue corresponding to MCCα R385 is part of a positively charged pocket for bicarbonate binding (36, 37).

For *MCCB*, we assume functional significance for the frameshift mutation S173fs(+1), the splice site mutation In5ac-1G→A and the missense mutation I437V, which alters splicing (Figure 5b). The remaining six *MCCB* missense mutations all change conserved residues and were the only coding alterations we found in sequencing the full-length ORF (Figure 3b). In expression studies, we showed that the *MCCB*-R155Q, -P310R, -S173L, and -E99Q alleles had no detectable MCC activity, whereas *MCCB*-V339M and -R193C had some residual activity, about 4% of the experimental control value (Table 3), when expressed in CG1-deficient reference cell lines. We identified V339M in two compound heterozygous Turkish probands (Table 2), the only patients in our collection with residual MCC activity in fibroblasts. Although 4% residual activity is at the detection limit of the standard MCC assay we used for the expression studies (27), these results are in accordance with the residual activity detected in fibroblasts of these patients with a modified MCC assay of increased sensitivity (3, 22). MCCα was reduced, but clearly present, in all CG1 cell lines in our biochemical detection of the biotin-containing α subunit (Figure 2). This suggests that the MCCα subunit is less stable when the β subunit is absent or defective.

Interestingly, we detected the MCCβ S173fs(+1), a T insertion, as one allele in a mildly affected Swiss compound heterozygote (20) and in an asymptomatic Mennonite homozygote from Lancaster County, Pennsylvania (Table 2). The ancestors of the Lancaster County Amish/Mennonite population originated from Switzerland (41) and may have brought this allele with them. Haplotype analysis will be necessary to confirm a founder mutation. Moreover, the Amish proband is homozygous for a different *MCCB* allele, E99Q. Thus, despite the small size and common origins of the Amish/Mennonite population in this region, there is allelic heterogeneity for MCC deficiency.

Combining our results and the published clinical reports (2–4, 19–25), we were not able to discern a phenotype-genotype correlation. Probands 010 and 015, homozygous for truncating mutations in *MCCA* or *MCCB* (Tables 1 and 2), have, in one case, no symptoms and, in the other, a mild phenotype with late onset and no residual damage (23). By contrast, probands 011, 001, and 002, homozygous for missense mutations *MCCA*-R385S, *MCCB*-S173L, and -E99Q, have a severe phenotype with early-onset, major neurological involvement and, in one case, a fatal outcome (Table 1) (2, 3, 24). Proband 016, an adult Amish patient homozygous for the same *MCCB*-E99Q, has only mild symptoms (4). Furthermore, the two Turkish patients with *MCCB*-V339M that have some residual MCC activity both have a severe phenotype. Taken together, these results suggest that factors other than the genotype at the

Table 2
MCCB mutant alleles

No.	Allele	Exon	Nucleotide change	Clinical phenotype[A]	Ethnic origin	Proband
1	R155Q	5	464G→A	Mild	Vietnamese	006
2	P310R	10	929C→G	Mild	Vietnamese	006
3	S173fs(+1)	6	518insT	Mild	Swiss/Mennonite[B]	004[C], 015[D]
4	I437V	14	1309A→G[E]	Mild	Dutch	003[C]
5	R193C	6	577C→T	Mild	Dutch	005
6	In5ac-1G→A		In5ac-1G→A	Mild	Dutch	005
7	S173L	6	518C→T	Severe	Turkish	001[D]
8	E99Q	4	295G→C	Severe/mild	Turkish/Amish	002[D], 016[D]
9	V339M	11	1015G→A	Severe	Turkish	007[C], 008[C]

[A]Mild: late onset, good recovery after acute attack, no or mild developmental delay; severe: onset in infancy, severe neurological involvement with severe developmental delay. [B]Detected by newborn screening. [C]Only one allele identified. [D]Homozygous. [E]Activates cryptic splice donor (Figure 5b).

Table 3
Expression[A] of *MCCA* and *MCCB* alleles

	Allele	Enzyme activity[B] (pmol/min/mg protein)			
		Experiment 1		Experiment 2	
		MCC	PCC	MCC	PCC
MCCA	Wild type	137	415		
	R385S	0	251		
	A289V	0	289		
	L437P	0	252		
	Vector	0	234		
MCCB	Wild type	170	548	110	474
	S173L	0	323	–	–
	E99Q	0	581	–	–
	V339M	7	336	–	–
	R155Q	–	–	0	359
	P310R	–	–	0	370
	R193C	–	–	6	373
	Vector	0	298	0	587
Control fibroblasts		318	345	325	436

[A]Transient transfection in SV40T-transformed reference CG1 or CG2 cell lines. [B]Numbers represent average of duplicates.

MCCA and *MCCB* loci (modifying genes, environmental variables) must have a major influence on the phenotype of MCC deficiency.

Since the widespread introduction of MS/MS to newborn screening, many new patients with MCC deficiency have been detected. Surprisingly, MCC deficiency appears to be the most frequent organic aciduria in these screening programs (4, 6–9) with an overall frequency of approximately 1 in 50,000. Studies of these prospectively identified individuals should provide insight into the factors that determine the phenotypic severity of MCC deficiency.

Note added in proof. We have recently learned that the molecular basis of MCC deficiency has also been identified by Gallardo et al. (2001, *Am. J. Hum. Genet.* **68**:334).

Acknowledgments

We thank A. Kohlschütter, U. von Döbeln, S. Berry, J. Smeitink, R.D. De Kremer Dodelson, W. Lehnert, U. Wiesmann, U. Wendel, W.J. Kleijer, B. Steinmann, B.T. Poll-The, D.H. Morton, and H.G Koch for referring fibroblasts of their patients, and J. Nathans for providing the human retina cDNA library and S. Muscelli for assistance in preparing the manuscript. M.R. Baumgartner, T. Suormala, and E.R. Baumgartner are supported by grants from the Swiss National Science foundation (32-40898.94 for T. Suormala and E.R. Baumgartner). R.N. Cole was supported by the American Health Foundation. D. Valle is an Investigator in the Howard Hughes Medical Institute.

1. Sweetman, L., and Williams, J.C. 1995. Branched chain organic acidurias. In *The metabolic and molecular bases of inherited disease*. 7th edition. C.R. Scriver, A.L. Beaudet, W.S. Sly, and D. Valle, editors. McGraw-Hill. New York, New York, USA. 1387–1422.
2. Bannwart, C., Wermuth, B., Baumgartner, R., Suormala, T., and Weismann, U.N. 1992. Isolated biotin-resistant deficiency of 3-methylcrotonyl-CoA carboxylase presenting as a clinically severe form in a newborn with fatal outcome. *J. Inherit. Metab. Dis.* **15**:863–868.
3. Lehnert, W., Niederhoff, H., Suormala, T., and Baumgartner, E.R. 1996. Isolated biotin-resistant 3-methylcrotonyl-CoA carboxylase deficiency: long-term outcome in a case with neonatal onset. *Eur. J. Pediatr.* **155**:568–572.
4. Gibson, K.M., Bennett, M.J., Naylor, E.W., and Morton, D.H. 1998. 3-Methylcrotonyl-coenzyme A carboxylase deficiency in Amish/Mennonite adults identified by detection of increased acylcarnitines in blood spots of their children. *J. Pediatr.* **132**:519–523.
5. Levy, H.L. 1998. Newborn screening by tandem mass spectrometry: a new era. *Clin. Chem.* **44**:2401–2402.
6. Naylor, E.W., and Chace, D.H. 1999. Automated tandem mass spectrometry for mass newborn screening for disorders in fatty acid, organic acid and amino acid metabolism. *J. Child Neurol.* **14**(Suppl. 1):S4–S8.
7. Smith, W.E., et al. 2000. Evaluation of elevated hydroxyisovalerylcarnitine in the newborn screen by tandem mass spectrometry. *Am. J. Hum. Genet.* **67**:292. (Abstr.)
8. Roscher, A.A., Liebl, B., Fingerhut, R., and Olgemöller, B. 2000. Prospective study of MS-MS newborn screening in Bavaria, Germany. *J. Inherit. Metab. Dis.* **23**:4. (Abstr.)
9. Wilcken, B., Wiley, V., and Carpenter, K. 2000. Two years of routine newborn screening by tandem mass spectrometry (MSMS) in New South Wales, Australia. *J. Inherit. Metab. Dis.* **23**:4. (Abstr.)
10. Samols, D., et al. 1988. Evolutionary conservation among biotin enzymes. *J. Biol. Chem.* **263**:6461–6464.
11. Wolf, B. 1995. Disorders of biotin metabolism. In *The metabolic and molecular bases of inherited disease*. 7th edition. C.R. Scriver, A.L. Beaudet, W.S. Sly, and D. Valle, editors. McGraw-Hill. New York, New York, USA. 3151–3177.
12. Jitrapakdee, S., and Wallace, J.C. 1999. Structure, function and regulation of pyruvate carboxylase. *Biochem. J.* **340**:1–16.
13. Lamhonwah, A.-M., et al. 1986. Isolation of cDNA clones coding for the *a* and *b* chains of human propionyl-CoA carboxylase: chromosomal assignments and DNA polymorphisms associated with *PCCA* and *PCCB* genes. *Proc. Natl. Acad. Sci. USA.* **83**:4864–4868.
14. Freytag, S.O., and Collier, K.J. 1984. Molecular cloning of a cDNA for human pyruvate carboxylase. *J. Biol. Chem.* **259**:12831–12837.
15. Abu-Elheiga, L., Jayakumar, A., Baldini, A., Chirala, S.S., and Wakil, S.J. 1995. Human acetyl-CoA carboxylase: characterization, molecular cloning and evidence for two isoforms. *Proc. Natl. Acad. Sci. USA.* **92**:4011–4015.
16. Lau, E.P., Cochran, B.C., and Fall, R.R. 1980. Isolation of 3-methylcrotonyl-coenzyme A carboxylase from bovine kidney. *Arch. Biochem. Biophys.* **205**:352–359.
17. Weaver, L.M., et al. 1995. Molecular cloning of the biotinylated subunit of 3-methylcrotonyl-coenzyme A carboxylase of *Arabidopsis thaliana*. *Plant Physiol.* **107**:1013–1014.
18. McKean, A.L., et al. 2000. Molecular characterization of the non-biotin-containing subunit of 3-methylcrotonyl-CoA carboxylase. *J. Biol. Chem.* **275**:5582–5590.
19. Mourmans, J., et al. 1995. Isolated (biotin-resistant) 3-methylcrotonyl-CoA carboxylase deficiency: four sibs devoid of pathology. *J. Inherit. Metab. Dis.* **18**:643–645.
20. Gitzelmann, R., et al. 1987. Isolated (biotin-resistant) 3-methylcrotonyl-CoA carboxylase deficiency presenting at age 20 months with sopor, hypoglycaemia and ketoacidosis. *J. Inherit. Metab. Dis.* **10**(Suppl. 2):290–292.
21. Beemer, F.A., et al. 1982. Isolated biotin-resistant 3-methylcrotonyl-CoA carboxylase deficiency in two sibs. *Eur. J. Pediatr.* **138**:351–354.
22. Wiesmann, U.N., Suormala, T., Pfenninger, J., and Baumgartner, E.R. 1998. Partial 3-methylcrotonyl-CoA carboxylase deficiency in an infant with fatal outcome due to progressive respiratory failure. *Eur. J. Pediatr.* **157**:225–229.
23. Tsai, M.Y., Johnson, D.D., Sweetman, L., and Berry, S.A. 1989. Two siblings with biotin-resistant 3-methylcrotonyl-coenzyme A carboxylase deficiency. *J. Pediatr.* **115**:110–113.
24. Steen, C., et al. 1999. Metabolic stroke in isolated 3-methylcrotonyl-CoA carboxylase deficiency. *Eur. J. Pediatr.* **158**:730–733.
25. Jurecki, E., and Packman, S. 1992. Nutritional therapy for beta-methylcrotonylglycinuria. *Metabolic Currents.* **5**:9–12.
26. Wolf, B., Willard, H.F., and Rosenberg LE. 1980. Kinetic analysis of genetic complementation in heterokaryons of propionyl CoA carboxylase-deficient human fibroblasts. *Am. J. Hum. Genet.* **32**:16–25.
27. Suormala, T., Wick, H., Bonjour, J.-P., and Baumgartner, E.R. 1985. Rapid differential diagnosis of carboxylase deficiencies and evaluation for biotin responsiveness in a single blood sample. *Clin. Chim. Acta.* **145**:151–162.
28. Old, S.E., and DeVivo, D.C. 1989. Pyruvate dehydrogenase complex deficiency: biochemical and immunoblot analysis of cultured skin fibroblasts. *Ann. Neurol.* **26**:746–751.
29. Nathans, J., Piantanida, T.P., Eddy, R.L., Shows, T.B., and Hogness, D.S. 1986. Molecular genetics of inherited variation in human color vision. *Science.* **232**:203–210.

30. Williams, K., LoPresti, M., and Stone, K. 1997. Internal proteins sequencing of SDS-PAGE-separated proteins: optimization of an in gel digest protocol. In *Techniques in protein chemistry*. D.R. Marshak, editor. Academic Press. New York, New York, USA. 79–90.
31. Smith, B.J. 1994. Chemical cleavage of proteins. *Methods Mol. Biol.* **32**:297–309.
32. Kennedy, R.T., and Jorgenson, J.W. 1989. Preparation and evaluation of packed capillary liquid chromatography columns with inner diameters from 20 to 50 μm. *Anal. Chem.* **61**:1128–1135.
33. Eng, J.K., McCormak, A.L., Ashley, L., and Yates, J.R.I. 1994. An approach to correlate tandem mass spectral data of peptides with amino acid sequences in a protein database. *J. Am. Soc. Mass Spectrom.* **5**:976–989.
34. Braverman, N., et al. 1997. Human *PEX7* encodes the peroxisomal PTS2 receptor and is responsible for rhizomelic chondrodysplasia punctata. *Nat. Genet.* **15**:369–376.
35. Leon-Del-Rio, A., and Gravel, R.A. 1994. Sequence requirements for the biotinylation of carboxyl-terminal fragments of human propionyl-CoA carboxylase alpha subunit expression in *Escherichia coli*. *J. Biol. Chem.* **269**:22964–22968.
36. Waldrop, G.L., Rayment, I., and Holden, H.M. 1994. Three-dimensional structure of the biotin carboxylase subunit of acetyl-CoA carboxylase. *Biochemistry.* **33**:10249–10256.
37. Thoden, J.B., Blanchard, C.Z., Holden, H.M., and Waldrop, G.L. 2000. Movement of biotin carboxylase B-domain as a result of ATP binding. *J. Biol. Chem.* **275**:16183–16190.
38. Saraste, M., Sibbald, P.R., and Wittinghofer, A. 1990. The P-loop: a common motif in ATP- and GTP-binding proteins. *Trends Biochem. Sci.* **15**:430–434.
39. López-Casillas, F., et al. 1988. Structure of the coding sequence and primary amino acid sequence of acetyl-coenzyme A carboxylase. *Proc. Natl. Acad. Sci. USA.* **85**:5784–5788.
40. Hendrick, J.P., Hodges, P.E., and Rosenberg, L.E. 1989. Survey of amino-terminal proteolytic cleavage sites in mitochondrial precursor proteins: leader peptides cleaved by two matrix proteases share a three-amino acid motif. *Proc. Natl. Acad. Sci. USA.* **86**:4056–4060.
41. Nolt, S.M. 1992. *A history of the Amish.* Good Books. Intercourse, Pennsylvania, USA. 318 pp.